

DARHT

Study Leader

Burton Richter

Contributors Include:

Henry Abarbanel
J. Mike Cornwall
Douglas Eardley
Richard Garwin
David Hammer
Russell J. Hemley
Raymond Jeanloz
Dan Meiron
Roy Schwitters

Consultants:

William Hermannsfeldt
Lloyd Multauf

Intern:

Brent Fisher

October 23, 2006

JSR-06-330

Approved for public release; distribution unlimited.

JASON
The MITRE Corporation
7515 Colshire Drive
McLean, Virginia 22102
(703) 983-6997

REPORT DOCUMENTATION PAGE

Form Approved
OMB No. 0704-0188

Public reporting burden for this collection of information is estimated to average 1 hour per response, including the time for reviewing instructions, searching existing data sources, gathering and maintaining the data needed, and completing and reviewing this collection of information. Send comments regarding this burden estimate or any other aspect of this collection of information, including suggestions for reducing this burden to Department of Defense, Washington Headquarters Services, Directorate for Information Operations and Reports (0704-0188), 1215 Jefferson Davis Highway, Suite 1204, Arlington, VA 22202-4302. Respondents should be aware that notwithstanding any other provision of law, no person shall be subject to any penalty for failing to comply with a collection of information if it does not display a currently valid OMB control number. **PLEASE DO NOT RETURN YOUR FORM TO THE ABOVE ADDRESS.**

1. REPORT DATE (<i>DD-MM-YYYY</i>) 22 October 2006		2. REPORT TYPE Technical		3. DATES COVERED (<i>From - To</i>)	
4. TITLE AND SUBTITLE DARHT				5a. CONTRACT NUMBER	
				5b. GRANT NUMBER	
				5c. PROGRAM ELEMENT NUMBER	
6. AUTHOR(S) Burton Richter, H, Abarbanel, J. Cornwall, D. Eardley, R. Garwin, D. Hammer, R. Jeanloz, D. Meiron, R. Schwitters, W. Hermannsfeldt, L. Multauf, B. Fisher				5d. PROJECT NUMBER 13069022	
				5e. TASK NUMBER PS	
				5f. WORK UNIT NUMBER	
7. PERFORMING ORGANIZATION NAME(S) AND ADDRESS(ES) The MITRE Corporation JASON Program Office 7515 Colshire Drive McLean, Virginia 22102				8. PERFORMING ORGANIZATION REPORT NUMBER JSR-06-330	
9. SPONSORING / MONITORING AGENCY NAME(S) AND ADDRESS(ES) US. Department of Energy National Nuclear Security Administration 1000 Independence Avenue, SW / Washington, DC 20585				10. SPONSOR/MONITOR'S ACRONYM(S) DP. NA-71	
				11. SPONSOR/MONITOR'S REPORT NUMBER(S)	
12. DISTRIBUTION / AVAILABILITY STATEMENT Approved for public release; distribution unlimited.					
13. SUPPLEMENTARY NOTES					
14. ABSTRACT JASON has been tasked by the NNSA with a review of progress on the second axis of the DARHT facility at the Los Alamos National Laboratory (LANL). DARHT 2 was declared complete in 2003 but, in subsequent testing, failed to achieve its design goals. A refurbishment project was begun in 2004 and it is this program that we were asked to review, and to answer 8 specific questions. Two days of excellent briefings by the staff of the 3 laboratories involved, LANL, Lawrence Berkeley National Laboratory (LBNL), and Lawrence Livermore National Laboratory (LLNL).					
15. SUBJECT TERMS Energetic materials, nuclear isomers, triggering, silver isomers, radioactivity					
16. SECURITY CLASSIFICATION OF:			17. LIMITATION OF ABSTRACT	18. NUMBER OF PAGES	19a. NAME OF RESPONSIBLE PERSON Dr. Joanna Ingraham
a. REPORT Unclassified	b. ABSTRACT Unclassified	c. THIS PAGE Unclassified			UL

Contents

1 EXECUTIVE SUMMARY	1
2 INTRODUCTION AND SUMMARY	3
3 INDUCTION CELL REFURBISHMENT	9
4 INJECTOR	13
5 BEAM DYNAMICS AND TESTING	17
5.1 Introduction	17
5.2 BBU Instability	18
5.3 Ion Hose Instability	19
5.4 Emittance Measurements	21
5.5 Conclusions on Beam Instabilities and Emittance	22
6 DOWNSTREAM TRANSPORT	25
6.1 Overview	25
6.2 Beam Induced Steering	26
6.3 Beam Defocus due to Ion Desorption	28
6.4 Ion Hose Instability	29
6.5 Resistive Wall Instability	31
6.6 Beam Spot Size	32
6.7 Testing on ETA-2	32
6.8 Conclusions on Downstream Transport	33
7 TARGET ISSUES	35
8 USER PROGRAM	37
A APPENDIX: NNSA's Charge to JASON	43
B APPENDIX: Briefers	45
C APPENDIX: Compensating for a lower DARHT 2 Current	47
C.1 The Detector	48
C.2 Pulse Width of the Four DARHT 2 Pulses	50

**D APPENDIX D: Simplified Simulation of DARHT
Edge Resolution**

51

1 EXECUTIVE SUMMARY

JASON has been tasked by the NNSA with a review of progress on the second axis of the DARHT facility at the Los Alamos National Laboratory (LANL). DARHT 2 was declared complete in 2003 but, in subsequent testing, failed to achieve its design goals. A refurbishment project was begun in 2004 and it is this program that we were asked to review, and to answer 8 specific questions. Based on two days of excellent briefings by the staff of the 3 laboratories involved, LANL, Lawrence Berkeley National Laboratory (LBNL), and Lawrence Livermore National Laboratory (LLNL), and our analysis of the issues, we answer the questions posed to us as follows:

1. Is there a sound technical basis for confidence in the refurbishment plans for the induction cells?

Yes. The rebuilding and testing program give high confidence that the problems associated with the induction cells are solved.

2. Is the approach to understanding beam stability issues and commissioning the accelerator technically sound?

Yes. The scaling laws used in the “scaled test program” are appropriate.

3. Are there unaddressed technical risks for the LINAC or ancillary and support equipment to meet design performance requirements for the LINAC?

Yes. The present injector cannot reach the original design goals, and there are uncertainties in the ability of a target to generate more than 2 satisfactory radiation pulses. There are well structured development programs aimed at curing both of these problems.

4. Is the technical approach to commissioning the downstream transport system sound?

Yes. As in our answer to question two, we find the scaling laws to be used in the test program to be appropriate. There is one small issue, back streaming of ions from the “dump target,” which needs further investigation.

5. What level of confidence exists that the 2nd axis will provide a useful multipulse capability? What risks remain in achieving the full 4-pulse capability at usable radiographic doses?

Confidence in two pulse capability is high. Target development is likely to be required to reach four pulse operations. Possible directions have been identified by the DARHT team.

6. Does the project execution plan follow a clear logic that addresses the activities needed to complete and commission the 2nd axis?

In general yes. However, fixes to the injector problems and possible target problems can only be developed after more testing.

7. In developing the final cost and schedule baseline project are there any significant shortfalls or gaps in the proposed technical scope or significant misestimates of resource requirements?

Possibly. This will depend on what is needed to address the injector and target problems. Based on what is known now, these fixes are not likely to be very costly.

8. Is there adequate planning to use the full capabilities of the two-axis multipulse radiographic system when the facility becomes available for experimental use?

No. The accelerator can support an aggressive operational program, but the infrastructure necessary to support the experiments themselves seems to be lacking.

2 INTRODUCTION AND SUMMARY

The Dual Axis Radiographic Hydro-Test facility (DARHT) has been under construction since 1988. The first axis, DARHT 1, has been successfully operational since 1999, but the second axis, DARHT 2, has been beset with difficulties. During a pause in the original construction project that occurred in 1995 as a result of a challenge to the project's NEPA approval, the second axis was redesigned to greatly improve its potential, increasing its energy modestly and adding the capability of taking four snapshots of the compression process during a test. This last improvement lengthened the acceleration pulse length considerably and made what was originally a straight forward advance in induction linear accelerator technology into a much more challenging project.

DARHT 2 was declared completed in 2003 with only minimal testing. Subsequent tests showed that the accelerator, as built, could not perform as required because of electrical breakdown in the accelerating modules. In December 2004 a refurbishing and commissioning program was approved by NNSA and our review has been charged with evaluating the status and prospects of the refurbishment plan (see Appendix A).

We had two days of briefings by Los Alamos, Livermore, and Berkeley staff (Appendix B). Charles McMillan, the LANL division director responsible for DARHT, and Ray Scarpetti, the DARHT project leader are to be commended for the well prepared presentations. It is clear that the DARHT project has the attention of higher laboratory management at LANL. In general we find that the DARHT group is pursuing a well thought out program of fixes and testing. As is not unexpected, the testing program is uncovering areas that need to be addressed if the performance specifications are to be met. Before getting to our overall evaluation, it is useful to go through the machine section by section.

The problem that led to the rebuilding program was the performance of the acceleration modules which would not stand the required voltage. Compounding the difficulty was the restricted space in the building and the requirement that the modules, much larger than those in DARHT 1, must fit into the same length space as the DARHT 1 modules.

Our review and comments on this issue are discussed in Section 3 of this report. We find that LANL has done a good job of analyzing and understanding the problems, improving the cell design and rebuilding the modules, and has instituted a good testing program. Six prototype rebuilt modules were subject to extensive testing at and above their design voltage before the start of the serial rebuilding program. The rebuilt modules are subject to a limited number of test pulses to identify infant mortality. Two modules of forty rebuilds have had troubles and have been successfully recycled. While the lifetime of the rebuilt modules cannot be determined until much more running time is accumulated, we conclude that one can have high confidence that the original electrical breakdown problems will not limit performance.

While the accelerating module problem seems to be solved, Section 4 discusses a new issue that has arisen that might limit performance. The electron gun in the injector section of the machine cannot deliver the specified beam current. The problems are that the cathode material is not capable of the required output at a temperature that will assure a reasonable cathode lifetime, and that the original cathode pulse voltage, 3.2 MV, might be too high for routine operation.

The DARHT 2 cathode, a type called a dispenser cathode, is quite different from that in DARHT 1 because of the longer pulse length. The 6.5 inch diameter cathode of DARHT 2 is required to emit a beam current density of about 10 A per square centimeter to meet the 2000 A performance goal. The present one cannot do so without heating to a temperature where its lifetime would be measured in hours. Since it is a major time consuming

operation to change a cathode, the problem needs to be addressed. There are existence proofs that dispenser cathodes can perform as required. However, their preparation is something of an art and the DARHT cathodes used a recipe for the material different from that used in successful cases such as the cathode in ETA-II at LLNL.

A fix that will allow a 2000 A beam will require better cathode material (new ones are on order), and either an increase in the electric field near the cathode (already designed) or going to a larger cathode. There is also a concern that the vacuum in the injector may be inadequate to allow proper cathode activation. A new cathode test stand exists at LBNL with a very good vacuum. When the first new cathode is delivered, it will be tested there. If it performs properly we suggest that it be then moved to the DARHT injector. Such a move requires careful control of the environment to which the cathode is exposed, but the process by which this can be done is known. Installation of the cathode that has been tested separates the issues of poor activation because of the DARHT vacuum environment from other possible injector problems.

In Appendix C we consider the potential impact on the hydrotest program if it is not possible to get a long-lived cathode that operates at 2000 A and operation is limited to around 1000 A with a longer pulse length for each of the four subpulses. We believe the effects are significant, but small enough not to compromise the mission.

Section 5 looks at the work to date on beam stability in the accelerating section of the machine. There are two potential problems; the Beam Break Up (BBU) instability, and the Ion-Hose instability. The concern is that the longer pulse length in DARHT 2 compared to DARHT 1 allows a longer growth time for an instability. Any effect that leads to a jitter in the beam at the target that is a significant fraction of the spot size can limit performance.

The DARHT team has designed a set of scaled tests that in principle

lead to the same growth rate as expected in the full machine while running at lower current and lower energy. We have reviewed their methodology and agree with their scaling laws. The work on scaled experiments, simulations, and theory gives confidence that beam jitter from these sources should be less than a few percent of the beam size at the target. Performance should not be limited from this source.

In Section 6 the transport of the beam from the end of the accelerator to the target is reviewed. The issues include beam induced steering in the kicker; the amount of beam defocus caused by background gas as well as gas desorbed from the septum as the beam is kicked; the possibility of ion hose instability in the downstream region; the existence of a transverse resistive wall instability; the quality of the spot size due to the interaction of the beam with the kicker; and the effect of gas emitted from the beam dump. Only this last one seems a possible problem which needs to be addressed further.

Because there are four pulses sliced out of a long electron beam (1.6-2 μ sec long), it may be that enough ions produced at the beam dump early in the kicker sequence may reach the main beam axis to defocus the last part of the long beam and interfere with the quality of the later pulses at the target. The DARHT group's analysis indicates that there will be no problem if the fractional ion emission per electron is below 1/10,000. What this number will be depends on the temperature and surface contamination of the beam dump. This issue can only be addressed in scaled experiments on DARHT.

In Section 7 the difficult target problem is discussed. The high beam intensity coupled with the required small size of the focal spot will give rise to target temperatures sufficient to vaporize most materials. In addition, ions from the target streaming back up the beam line can defocus the incoming beam and prevent achieving the required good focus at the target. Light ions, like water adsorbed on the target surface, give the most problems within one of the short pulses, since they can stream back the furthest. Heavier ions

produced from earlier pulses in the four pulse chain can remain around and affect later ones.

The DARHT group has studied the problem through simulations and experiments at both DARHT 1 and ETA-II. There are several alternate schemes that might be used.

The target problem has been addressed experimentally to the point where one can have high confidence in the delivery of two out of the four pulses, and lower confidence that it will work for all four. The DARHT team has identified several other approaches that are backups to the baseline scheme. We have pointed out where advanced materials that are not unreasonably difficult to fabricate could help.

In conclusion, we have high confidence that the current baseline approach to target design will deliver two x-ray pulses, but lower confidence that all four x-ray pulses will meet requirements. Promising approaches exist for a more capable target design, but will require further experimentation and development. The Scaled Accelerator Test is of key importance. Only experiment will determine definitively which approach will work.

Section 8 looks at the potential user program. Limitations on the frequency of experiments are not likely to come from the accelerator systems, which should have no problem sustaining a rate of at least one shot per week. Limitations are much more likely to come from inadequacies in the infrastructure required to support the experiments themselves. We suggest that planning for the dual axis experimental program should start soon and involve, from the beginning, the experimenters, the weapons designers, and the facility managers. In this way the requirements for an expanded program of tests can be developed early enough to allow implementation by the 2008 start time of dual axis operations.

3 INDUCTION CELL REFURBISHMENT

As an induction accelerator, DARHT 2 depends on the performance of many (74) essentially identical induction cells that sequentially add energy to the beam produced by an injector. They must be designed to transmit the beam without distortions so that at the end of the accelerator, it can be focused to a small spot at the x-ray conversion target. Issues of concern include:

- Supplying sufficient energy at each cell gap to achieve the total beam energy goal of 17 MeV;
- Maintaining voltage for at least $1.9 \mu\text{s}$;
- Limiting beam breakup instabilities caused by beam-induced fields in the acceleration gaps; and
- Maintaining the flatness of the voltage waveform to $\pm 1\%$ over the $1.5 \mu\text{s}$ duration.

The major problem identified during the DARHT commissioning phase after formal completion of the construction project in 2003 was the failure of the cells to hold off the design voltage, which is required to achieve the beam energy specification for the accelerator. On evaluating damaged cells it was found that there was arcing in various places in the oil region of the cell, a breakdown in the vacuum region across the oil-vacuum insulator, and arcing between the cathode and anode. Taken together, these problems reflected serious design deficiencies that would probably have been diagnosed and remedied during the original construction phase but for deficiencies in the testing program.

In the process of improving the cell design, extensive work was done with 2D computer modeling that revealed regions with higher than expected

fields. Design changes were made to reduce fields to levels that would be conservative under intended accelerator operation. The changes to the cell design and preparation are summarized below:

- Extending the length of the cells by 1 inch with increased metglas core-to-HV plate spacing and use of longer HV-to-ground spacers;
- Modifications to reduce the effects of capacitive coupling between the metglas cores and ground; and
- Inclusion of a high density polyethylene spacer between metglas cores, replacing multiple Mylar spacers that trapped pockets of air.
- Cathode and oil-vacuum insulator modifications to reduce fields on the insulator and prevent flashover.
- Diodes added to PFNs to clamp cell reversal voltages.
- Oil fill procedure changes to use multiple fills to clean away debris, to degas the oil prior to final fill, and to fill under vacuum to eliminate air pockets.

The fixes were also analyzed by 2D modeling and verified by experimentally evaluating the new cell design. Evaluation included pulsed testing of 6 cells for about 190,000 pulses at or above the 200kV design operating voltage. In addition, a refurbished cell was tested with beam at 235 kV for hundreds of pulses by including it on long-pulse beam stability tests (for which otherwise non-refurbished cells were used). Beam tests also included intentional beam spilling centered on the refurbished cell. In all of these tests, there were no faults, which validated confidence in the refurbished design.

Two refurbishment lines were set up to rebuild all of the cells, with improved quality assurance procedures to ensure the integrity of the rebuild effort. A test program was established to evaluate all rebuilt cells. The

testing entails subjecting each refurbished cell to 1000 continuous shots at 250 kV to identify any infant mortality problems before cells are installed on the accelerator. So far 2 of 38 refurbished cells have failed the tests and were returned for further rebuild. One failure was understood (a chip under an insulator), and the other was thought to be caused by a bubble in the oil, though that was not firmly established. The experience with these cells is being applied to reduce infant mortality. In addition, of the refurbished cells, 26 are operating on a scaled version of the accelerator that began operation in April and will continue for nearly a year to address beam and target issues. The scaled accelerator tests have been used to establish that the new cells meet the composite voltage flatness requirement for achieving the required focal spot size on the finished accelerator, one of the major requirements of the refurbished cells. The remaining cells will be rebuilt, tested according to the established protocol, and stored until the full accelerator is assembled.

In our opinion, the program put in place after problems with the cells were discovered has led to a much improved understanding and an improved cell design. The testing program on prototype refurbished cells, including tests with beam, was adequate to establish a basis for proceeding. The refurbishment program appears to be well designed, with attention paid to quality control procedures. The testing protocol for refurbished cells should be adequate to correct infant mortality problems. We have some concern that completed modules will be held until well into 2007 before being installed on the accelerator, but have no suggested alternative, given the importance of planned scaled accelerator tests. Additional testing of refurbished cells on the scaled accelerator will add further useful data on cell performance with beam, though a full determination of cell life with beam will be determined only on the fully recommissioned accelerator. In summary, the cell refurbishment and testing program as described by the project team gives high confidence in a successful outcome.

4 INJECTOR

Present cathode performance is inadequate to deliver the required beam current on target with reasonable cathode lifetime. The cathode that is operating at the time of this review is running at about 1140 C and emitting about 1000 A. This gives an average emission density of about 4.3 A/cm². It is presently operating at the space charge limit, which is the way it was designed to run. To get to the 2000 A needed to meet the DARHT design goal requires higher cathode temperatures and higher electric fields in the gun region. However, diagnostics show that even with sufficiently high electric fields, in order to emit close to 10 A/cm², as needed to achieve 2000 A, the present cathode would require much too high an operating temperature to survive for any reasonable time. This is a major problem since it requires weeks to make any changes in the injector, including just replacing the cathode. The reasons for the current performance limitations are not yet fully understood.

Thermionic cathodes are used in high power vacuum tubes and in accelerator injectors. In DARHT 1, a type called a “velvet cathode” is used to create a plasma from which the required electrons are extracted during the high voltage pulse. However, such cathodes do not perform well for long pulses such as the two-microsecond DARHT 2 pulse. In power tubes or accelerators designed for a long pulse or for continuous operation, a tungsten disk is used with certain impregnations and coatings to reduce the work function and permit high current density. The impregnation material, usually barium, is mixed into the tungsten granules before the cathode disk is compressed and fired. Care is then taken during machining to avoid closing over the grains so that the barium is allowed to migrate from the interior. Finally, one of a variety of coatings is applied to further enhance the emission.

These coatings are notoriously sensitive to environmental conditions and so must be heated carefully to drive out moisture and then must be protected from contaminants in the vacuum system. Even a good vacuum may have constituents that are detrimental to cathode performance. The choice of coating is affected by the expectation that the cathode will operate in an induction linac, with some environmental compromises, as contrasted to a vacuum tube that has only metal seals and can be baked at high temperature for several days. DARHT, with O-ring seals and large tanks filled with oil cannot be baked. The injector region also has a great number of surfaces, some of which are designed to move, and all of which are sources of gas contaminants. During operation, the cathode is heated to provide sufficient thermal energy to allow the electrons to escape the surface. The heating must be controlled to avoid causing the barium to evaporate too quickly and especially, to preserve the coating.

The present cathode is operating at about 1140 C which is somewhat on the high side but not dangerously so. However, even at this elevated temperature it does not produce the expected current density. A diagnostic process that can show what temperature is needed for higher current density can be used to develop what is known as a Miram curve. The Miram curve for this cathode indicates that to reach 10 A/cm², the cathode would need to operate at above 1200 C. At such a level, cathode lifetime would be measured in hours. The actual impregnations and coating recipes for the present cathode are not especially clear to us at this time, but they are clearly not what is desired for this application.

We note that there is an existence proof for appropriate operation in a cathode mounted on the ETA-II linac at LLNL. This cathode has operated for a number of years and is reported to emit 16 A/cm². Only recently has the recipe (impregnation and coating) been found that was used on the ETA-II cathode. There is great interest in reproducing the ETA-II recipe for a new

cathode for DARHT. Two have already been ordered and the first will be delivered in early August, 2006.

It is worth noting that there are other applications that demonstrate the ability to produce the kind of performance required here. For example, there is extensive experience at the Stanford Linear Accelerator Center with 60 MW klystrons with a pulse length similar to the DARHT 2 specification. These operate for thousands of hours without cathode failures. They use cathodes that are similar to the ETA II cathode.

Compounding the problem, the DARHT electron gun is not to be operated at the original design voltage. Out of concern for possible damage to the injector, the injector column has been operated at about 2 MV as compared to the design level of 3.2 MV. At this level, it is not possible to get much more current from any cathode. At 2.5 MV, which is a level that the DARHT group seems comfortable with, the space charge limited current given the design geometry would be about 1.4 kA. A modification to the design has been developed that would move the cathode closer to the anode (by 3 inches out of the present 13 inches) and would raise the design microperveance to 0.5, resulting in space charge limited operation at 2 kA with an average emission density of about 10 A/cm².

The LBNL, part of the DARHT collaboration, has built a cathode test stand that would operate up to 50 kV and would permit activation and testing of cathode samples. It would especially allow determination of the Miram curve to predict the temperature that will be required to operate at higher current density. The cathode that is now being procured, with the ETA-II recipe, will be first tested on the LBNL tester. Assuming that it performs as expected, it should be moved to DARHT. Careful control of the cathode's environment is required but the process is known.

As mentioned earlier, the vacuum conditions in the DARHT injector are also a concern. However, the experience with ETA-II is making the

DARHT team optimistic that the new formulation, and the cathode move, will serve to provide a cathode with the needed performance and lifetime to meet the DARHT requirements. Once the new cathode becomes available, it is important that it be tested in place to see if the environment in the injector is a problem. The current plan is to install the new cathode and reduce the cathode-anode spacing to increase the field in February of 2007. The delay will allow the completion of the target test program which we agree should have priority. Should there be an interruption of the test program in the fall, the cathode might be installed early.

If it should turn out that the 2000 A goal cannot be reached, there are remedial options. One which is analyzed in Appendix C to this report is to operate with somewhat longer pulses on the target so that the required x-ray flux can be delivered at a lower beam current. Another option is to replace the present 6.5 inch diameter cathode with one that is closer to the originally designed 8 inch diameter. This would be a more significant hardware alteration than just moving the cathode closer to the anode. It would however reduce the emission current density required to about 6.5 A/cm².

5 BEAM DYNAMICS AND TESTING

5.1 Introduction

In the DARHT main accelerator, two instabilities are thought to be potentially important. The first is the beam break-up (BBU) instability, which in its simplest form occurs for a beam of particles of a single charge propagating in an accelerating structure, and interacting with a mode of the accelerator cavity. The second is the ion-hose instability, which is driven by the interaction of the electron beam with a low-energy ion channel arising from beam ionization of neutral gases in the imperfect vacuum of the accelerator. These potential instabilities for DARHT 2 have been studied experimentally with an accelerator configuration significantly different from the planned final configuration in both energy and current. The table below (taken from [1]) shows the differences. Since the strength of these instabilities depends on both current and energy (as well as, for the ion-hose instability, the neutral-gas pressure in the accelerator), for an experimental test of the instabilities to be meaningful for the full-scale DARHT 2 accelerator it must be shown that the expected dependences on the parameters of Table 1 are realized. (The BBU instability depends on the accelerator cell geometry and physical properties, which are the same for the full and the test accelerator configurations.) Then it will be permissible to extrapolate the currently-available test results to the full-scale accelerator.

Aside from these potential instabilities, an important measure of beam dynamics and accelerator performance is emittance. For DARHT 2, emittance, which measures a product of beam spot size and angular spread, is not as important as the spot size at the target, which largely controls the

Table 1: Beam-dynamics test accelerator compared to the full-scale DARHT 2 accelerator (based on [1])

	Stability tests	Final
Beam current (kA)	1.1-1.3	2.0
Pulse length (μsec)	1.6 flat	1.6 flat
Diode voltage (MV)	2.5	2.5
Injector cells	$6 \times 90 \text{ keV}$	$6 \times 175 \text{ keV}$
Injector cells (MeV)	0.54	1.05
Injector energy (MeV)	3.0	3.6*
Installed cells	50	68
Active cells	$39 \times 100 \text{ keV}$	$68 \times 200 \text{ keV}$
Final energy (MeV)	6.9	17.2

* The entry in the equivalent table in Ref. 1, 4.3 MeV, reflected the original design diode voltage of 3.2 MeV. The present plan calls for a value of 2.5 MeV, as stated in the table above.

size of the X-ray source. Currently there are significant differences between emittances as measured by different techniques. We will discuss this issue and our suggestion for its resolution.

5.2 BBU Instability

In this instability, an off-axis beam couples to dipole modes of the accelerator cells, generating electromagnetic fields in these modes. These fields then further deflect the beam, generating more dipole radiation; ultimately the beam can be disrupted. The instability is cumulative, meaning that the instability growth rate grows linearly with the number of cells. The BBU instability occurs under a wide variety of conditions, but it has been argued [2] that various types of BBU are classified by just two dimensionless parameters. For the DARHT 2 regime, the relevant dimensionless parameter occurs in the instability growth rate Γ , which scales as [1]

$$\Gamma \sim INZ_{\perp} \left\langle \frac{1}{B_z} \right\rangle \quad (5-1)$$

where I is the beam current, N the number of cells, Z_{\perp} the transverse impedance of the cells, and $\langle 1/B_z \rangle$ is the average inverse longitudinal magnetic field. In addition, the time to reach maximum amplification scales with the cavity Q .

The Los Alamos group studied the BBU instability in the scaled accelerator, where the current and number of cells differs from that of the full DARHT 2 accelerator. They confirmed the scaling of growth with magnetic field by varying the field, and confirmed the variation with the number of cells by measuring growth at various points along the accelerator. Additionally, they measured the transverse impedance. By varying the magnetic field they were able to tune the growth rate to that expected in the full DARHT 2 accelerator, and found a beam displacement less than 2% of the beam radius. Further confidence comes from BBU simulations using the envelope code LAMDA, which generally confirm the scaled-accelerator experiments.

5.3 Ion Hose Instability

In this instability, an ion channel along the electron beam is formed by beam-electron ionization of residual gas atoms in the accelerator; low-energy electrons so formed are expelled by the beam electric field. If for some reason a displacement arises between the electron beam and the ion channel, both the ions and the electrons begin to oscillate at their characteristic frequencies. For the electrons this is the betatron frequency, but the much heavier ions (effectively heavier by a factor of about 150 times the ions mass number in the scaled accelerator) oscillate at a much smaller frequency. Because the ions are so heavy the wavelengths of the oscillations of electrons and ions are nearly the same and electron oscillations are nearly spatially resonant

(unstable). In DARHT 2 the ion oscillations go non-linear first, which causes a reduction in the ion-hose growth rate [3].

Here we discuss this instability semiquantitatively. It is discussed analytically in Section 6.4 in the context of the beam transport to the target.

R. J. Briggs has done an unpublished calculation of the ion-hose growth rate for DARHT 2 conditions, where the prevailing vacuum might lead to an ion density $10^{-4} - 10^{-3}$ of the electron beam density. He calculates the following scaling for the growth rate at a distance L along the accelerator:

$$\Gamma \sim I\tau_{pulse}L \left\langle \frac{p}{B_z R^2} \right\rangle \quad (5-2)$$

where, as before, I is the electron current and B_z the longitudinal magnetic field. Here τ_{pulse} is the length of the pulse, p the neutral gas pressure, and R is the beam radius¹. The dependence on $p\tau_{pulse}$ reflects the production of ions by the electron beam. Ion-hose simulations have been done for the DARHT 2 regime in [3], where an estimate is given for the fraction f of ions produced per beam electron of $f \simeq 0.9 \times 10^9 p[\text{torr}]\tau_{pulse}[\text{sec}]$, or about 3×10^{-4} at a pressure of 2×10^{-7} torr. Briggs' linear calculation is confirmed by these numerical particle-in-cell simulations using the LSP code [3], which go further into the non-linear regime and show that stabilization can occur with a small electron beam displacement and an ion channel displacement several times larger, because the amplitude dependence of the ion oscillation frequency changes it enough to go out of spatial resonance with the electrons.

Obviously, with no ions there is no ion-hose instability, so the main mitigation measure is to reduce the pressure. The Los Alamos group [1] has studied the dependence of ion-hose scaling effects in the scaled-accelerator configuration by varying the pressure, and have also validated Briggs' calculated growth rate. At a pressure as high as 2×10^{-7} torr, only slight evidence

¹Note that the beam radius itself may depend on scaling variables such as the ratio of current to the Alfvén current, or $I/\beta\gamma$, where β and γ are the usual relativistic factors. Effectively, this is the ratio of beam current to beam energy, which—by design—does not change much between the full and the scaled accelerator

of electron-beam motion due to ion-hose effects was seen. When the pressure was scaled up by a factor of 6, the instability was clearly present. Ion-mass scaling of the dominant frequency (not growth rate) was confirmed by using Xe and Ne ions, and Briggs' prediction of saturation of the instability as a function of accelerator conditions was also verified nicely. As with BBU, parameters, especially pressure, were set in the scaled accelerator to yield the same growth rate as in the full DARHT 2, and motion was no more than 2% of the beam radius; in fact, when the pressure was increased by a factor of 6 the motion was restricted to 10%.

As a mitigation measure, in the full DARHT 2 accelerator there will be an interlock preventing the accelerator from operating if the pressure exceeds 10^{-7} torr.

5.4 Emittance Measurements

Two methods have been used to measure emittance at the scaled accelerator, as used for the beam dynamics studies, and a third one is proposed. The first method uses the focal scan technique, in which a focusing magnet is used at the accelerator exit to focus the beam onto a Cerenkov radiator; the Cerenkov radiation was captured with a streak camera. An envelope code is used to back out the emittance from the known beam size and focusing strength of the magnet, as the focusing strength is varied. The second method uses a "pepper pot" near the injector, where the electron beam is at low energy and space-charge effects are strongest. In this method the beam passes through a series of holes in a screen, forming several beamlets, each of which is imaged on an imaging detector. The emittance can be calculated from the intensity profiles of the beamlets.

The focal scan method yielded an emittance of about 600π -mm-mr, while the pepper pot method yielded an emittance about 50% higher. This

higher emittance at the front end, rather than the naive expectation that the accelerator could add emittance during the beam transit, may well come from loss of the highest transverse energy components of the beam after the location of the pepper pot, which would reduce both current and emittance. In any event, what counts for DARHT 2 facility is not the emittance but the beam spot size at the target. There is no specific requirement for emittance for this reason, but the requirements on beam spot size are being met, according to the emittance studies.

The third proposed method to measure emittance would use polarized optical transition radiation (OTR) detectors. To avoid damaging these, the beam must be fairly large spatially and thus have a small angular divergence. As of now the Los Alamos people have little experience with OTR emittance measurements, and they [1] have only an upper limit on emittance of 1500π -mm-mr.

Among these emittance-measurement techniques we believe that the focal scan method is preferred, since the pepper pot method could potentially interfere with the beam and hence the emittance measurement, and OTR, which depends on very accurate measurements of small angles and is sensitive to background effects, is not yet well-developed at Los Alamos.

5.5 Conclusions on Beam Instabilities and Emittance

Our general conclusion is that, based on scaled tests and studies of scaling laws, the instabilities are not a serious threat. The combination of experimental work on a scaled accelerator, simulations, and instability theory provide convincing evidence for this conclusion. There is good evidence that beam displacement as a percentage of beam radius may actually be around 2% at DARHT 2, well within the required 10%.

Emittance is not really the figure of merit for the DARHT 2 accelerator; what matters is the beam spot size on the X-ray target. However, there has been a campaign to measure emittance as it is important information on accelerator function. We conclude that the highest-confidence method for acquiring emittance data is through the focal scan method used at Los Alamos. This method has given the smallest emittances of the methods used and is made at the exit end of the accelerator, where it really matters.

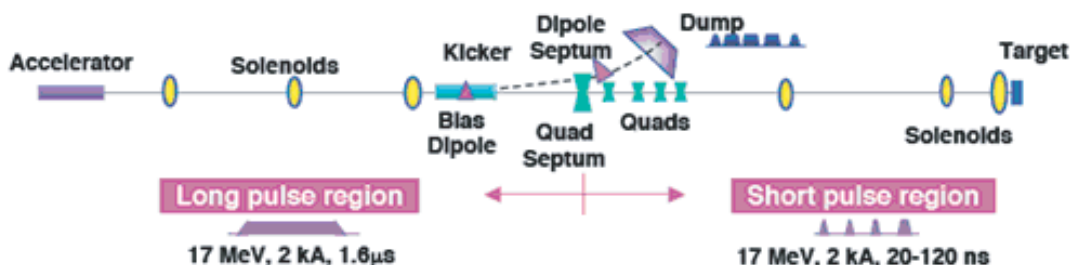
6 DOWNSTREAM TRANSPORT

6.1 Overview

The downstream transport for the final DARHT 2 configuration refers to the design and operation of the crucial beam processing elements located between the end of the accelerator and the target. These elements are used to slice the beam temporally into a set of pulses and then to direct these pulses onto the X-ray target.

The downstream transport consists of a straight section with solenoidal focusing followed by a kicker combined with a bias dipole magnet and sextupole element used to divert the beam into a beam dump. The “dump” mode with the kicker off and the beam diverted to the dump is the standard operation. When portions of the beam are to be directed to the target to produce X-rays, the kicker is pulsed on and the beam proceeds forward to the target for the required pulse length. A set of quadrupole magnets and solenoids are used to transport and focus the beam at the target.

A schematic of the downstream system (From Caporasso and Chen [7] is shown below.



The major issues that need to be addressed in proper design of the downstream system are the following:

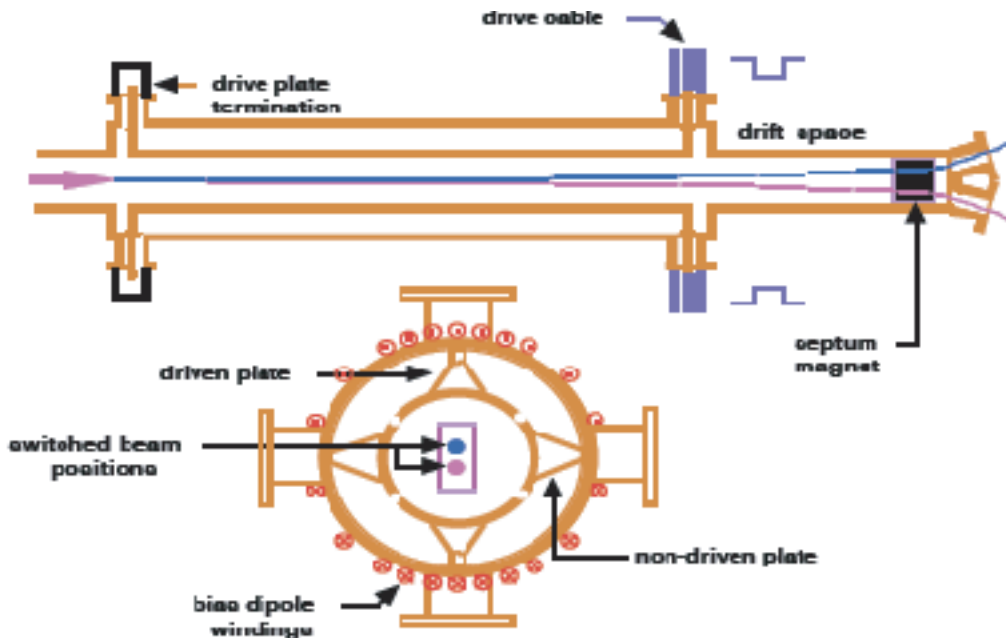
1. Beam-induced steering in the kicker;

2. The amount of beam defocus caused by background gas as well as gas desorbed from the septum as the beam is kicked;
3. The possibility of ion hose instability in the downstream region;
4. The possible existence of transverse resistive wall instability; and
5. The possible degradation of the spot size due to the interaction of the beam with the kicker.

In the following we will review these issues and provide assessments of how well these issues are being addressed.

6.2 Beam Induced Steering

In order to kick the beam a stripline system is used in combination with a bias magnet. The configuration is shown below from (Ref. [7]):



To 'kick' the beam, a high voltage pulse is applied to the kicker stripline which cancels the DC field of the bias magnet.

The beam current is sufficiently large to induce substantial voltages and currents back on the strip transmission lines. These effects are significant and so must be thoroughly understood and included in beam dynamics calculations. A theoretical model of this effect has been constructed to compute the asymptotic beam deflection due to the beam induced field. The asymptotic beam deflection is related to the geometry and impedance of the stripline system. Provided the ratio of the beam current to a facility-specific critical current is sufficiently small, a linear approximation can be used to predict the beam deflection and thus the amount of beam-current-induced steering. The LLNL group has shown that these results (including the linear approximation of the beam deflection) are consistent with more detailed particle transport simulations. These relations have been tested on the ETA-2 accelerator at LLNL.

From this we see that beam-induced steering depends on the ratio of beam current to the critical current. For DARHT 2 at 17 MeV beam energy the critical current is 11.3 kA. Thus the ratio of beam current at 2kA to critical current is reasonably small and so the various calculations should be predictive. Even for relatively high ratios of the beam to critical current, it is possible to control the beam deflection through the application of a feed-forward control system. LLNL has demonstrated this capability for current ratios as high as 0.45.

Finally, a solid state pulser system for the kicker has been developed which provides excellent pulse width and amplitude control. The system can reliably provide 1-4 pulses with a spacing of at least 400 nsec. The required dose format is achieved by varying the individual pulse widths. The performance of this system has been demonstrated by comparing its output with a predicted pulse format on ETA-II.

6.3 Beam Defocus due to Ion Desorption

There remain a number of issues to be explored as regards long pulses. For example, there is a possible concern that gas desorption from the septum knife edge may play a deleterious role at the higher currents of the DARHT accelerator. This has been addressed in several ways. First, the quadrupole magnet upstream of the septum has been designed to have a large bore so as to maximize the septum acceptance. This acts to expand the beam so that it enters the dump with a lower energy density.

An additional concern is that ions that are desorbed from the graphite dump can stream back and affect the focus of the beam at the dump. Particle simulations of the beam-dump interaction using the LSP code have made it possible to assess the effect of desorbed H^+ ions as they stream back from the dump. These simulations indicate that if the yield of H^+ ions is less than 10^{-4} , the beam focus is essentially unaffected. In order to mitigate these potential problems, it has been proposed to bake the beam dump so as to lower the yield of H^+ as well as to increase the beam size. Experiments performed at DARHT-I have shown that the yield for such ions is within the acceptable range.

There is some concern over the conditions that will hold when the four pulses are created. The DARHT briefing material indicates that these ions reach the septum at roughly 350 nsec with a speed v relative to the speed of light c , $\frac{v}{c} \equiv \beta$ of 0.03 if the electron beam current is 2kA. This is said to be a worst case, but the DARHT 2 requirements call for beam duration of 1.6 μ sec. The individual pulses are 20 to 120 nanosecond in duration. In the roughly 300 ns intervals between pulses the beam goes to the dump and generates the H^+ ions. It is then switched to the target by the kicker. We were not shown integrated simulations that examine the effect of this cyclic switching over all four pulses and its impact on the number and spatial distribution of ions generated during the time the beam is repeatedly kicked.

An analysis using particle simulation provides an estimate of beam loss as the beam sweeps over to the target from the dump. It would be beneficial to perform an beam dump region simulation that includes the full operating condition of four pulses to insure that the relatively long pulse time does not affect the earlier conclusions about beam defocus due to ion desorption.

6.4 Ion Hose Instability

Another concern is the ion hose instability that was discussed in Section 5.3 in the context of the accelerator region. To reiterate, the beam electrons create positive ions by impact with residual gas atoms in the vacuum system. The macroscopic interaction of the beam and the ion column can destabilize the beam and, as a result, transverse deviations of the beam could grow.

Following McCarrick [8], if the ion column transverse displacement from the drift pipe axis in the x-direction at some point along the electron beam is $x_i(t, z)$, then it satisfies the equation of motion

$$\frac{\partial^2 x_i(t, z)}{\partial t^2} = \omega_0^2(x_b(t, z) - x_i(t, z)) \quad (6-3)$$

where

$$\omega_0^2 = \frac{Zq_i I_b}{2\pi\epsilon_0 A m_p r_b^2 c} \quad (6-4)$$

and $x_b(t, z)$ is the transverse displacement of the beam from the center of the drift pipe, q_i is the ion charge, Z is the ion charge state, A is the atomic mass number, m_p is the proton mass, and I_b is the beam current.

The beam displacement also satisfies such an equation, and in coordinates moving along with the beam, called z , we have for the beam displacement

$$\frac{\partial^2 x_b(t, z)}{\partial z^2} = \alpha\omega_0^2(x_i(t, z) - x_b(t, z)) \quad (6-5)$$

where

$$\alpha = \frac{f A m_p}{Z \gamma m_e}, \quad (6-6)$$

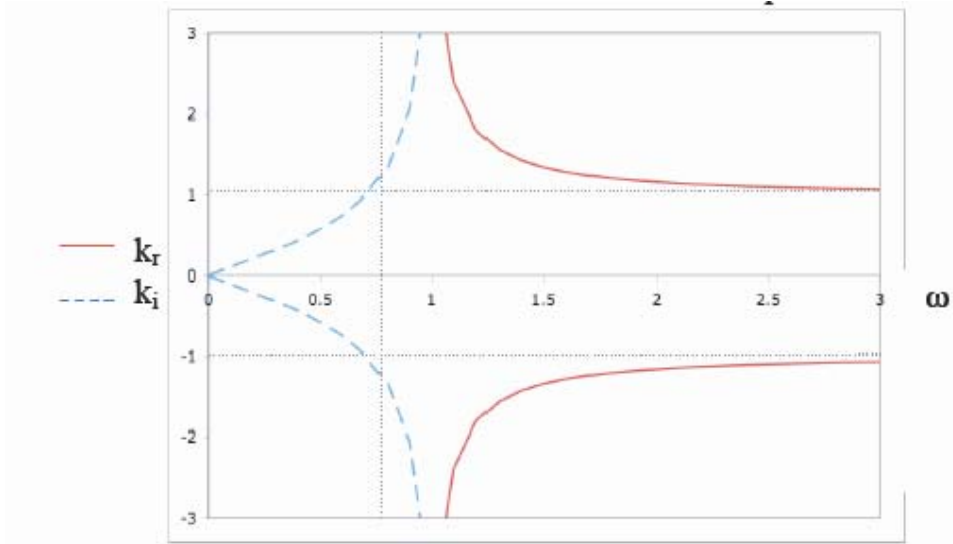
f is the neutralization fraction, and γ is the beam energy divided by $m_e c^2$.

Scaling time by $1/\omega_0$ and space by $\frac{\beta c}{\sqrt{f}}$, we have

$$\begin{aligned}\frac{\partial^2 x_1(t, z)}{\partial t^2} &= (x_b(z, t) - x_i(t, z)) \\ \frac{\partial^2 x_b(t, z)}{\partial z^2} &= (x_i(z, t) - x_b(t, z))\end{aligned}$$

which leads to the dispersion relation $1 = (1 - \omega^2)(1 - k^2)$ for solutions proportional to $\exp(i(kz - \omega t))$.

One can see from the graph of the real and imaginary part of the wavenumber versus frequency (left), that since an initial disturbance will contain all frequencies, there will be an imaginary part leading to growth in the disturbance.



McCarrick [7] reports calculations showing that if the residual gas pressure is lower than about 10^{-6} torr, the transverse beam growth in settings simulating DARHT 2 conditions will not be important. The design pressure is 1.5×10^{-7} torr, so one can conclude from these calculations that over the length of order 12m of the transport system the beam growth from this instability will not be troublesome. The growth of an initially small beam, 5 mm in the calculations, is more than that of a larger beam, 2 cm, in these

calculations. Quantitatively one estimates that the beam envelope in the transport pipe expands as $x_0(1 + \mu \sin(\frac{\pi z}{L}))$ with $\mu \approx 5$ at the design pressure [5]. The number of e-foldings of the ion-hose over the length of the transport section for this value of μ is far less than 0.1 [9].

6.5 Resistive Wall Instability

Another instability in the transport system after the accelerator is associated with the fact that the relativistic electron beam induces currents in the transport pipe which set up fields in the pipe cavity that affect the beam passing later in the pipe. For a single relativistic charge this is insignificant, but for a long beam, fields induced by the passage of the head of the beam may strongly affect the tail of the beam. The fact that the field induced is out of phase with the head of the beam and is frequency dependent means that instability may be induced.

The equation of motion for a transverse displacement $x(t,z)$ has the general form $\frac{\partial^2 x(t,z)}{\partial z^2} + \omega_0^2 x(t,z) = \int_0^t W(t', x(t', z)) dt'$, where the “wake function” W represents the effect of early arriving beam on later arriving beam through the induced fields in the beam pipe wall. This equation leads to a dispersion relation which may have positive imaginary wake function solutions leading to growth in the amplitude of $x(t,z)$. Estimates for this growth in the DARHT 2 setting for a beam of 2 kA and $2\mu\text{s}$ duration indicate that in a region with two downstream 3m long stainless steel drift pipes of diameter 16 cm, the growth length is 6.4 m for a 2 kA beam. Using Al pipes will increase this growth length by about a factor of three.

6.6 Beam Spot Size

The switching of the beam due to the kicker can also have a deleterious effect on the spot size when the beam impinges on the X-ray target. This has been dealt with by using the final solenoids to reduce the smear of the beam spot by tuning its envelope so that the target location corresponds to a betatron node. Simulations using the TRANSPORT PIC code as well as experiments on the ETA accelerator indicate that beam spot smearing can be controlled to an acceptable level by means of this technique.

6.7 Testing on ETA-2

A significant amount of testing has been performed on the ETA-II accelerator at LLNL. ETA-II is a 5.3MeV induction linac that provides a beam at 2kA for 50nsec at 1 Hz. The ETA-II tests have made it possible to assess the importance of many design issues prior to the commissioning of the DARHT 2 accelerator. The status of these experiments, their implications for DARHT 2 and the remaining issues that will be explored during the scaled accelerator tests are shown in the table below extracted from the presentation of G. Caporaso (Ref. [7]).

<u>Issues</u>	<u>ETA-II</u> <u>Experiment</u>	<u>Remaining</u> <u>Issues</u>	<u>Scaling</u>
Transport and Kicker			
Kicker operation & control system	√	4 pulses, 1.6 μs	none
Septum gas desorption	√	4 pulses, 1.6 μs	$I n_p \tau_{\text{kicker_switch}}$
Beam induced kicker steering	√	1.6 μs	$I/\gamma\beta$
Background gas focusing		1.6 μs	$I/\gamma\beta$
Ion-hose instability suppression		1.6 μs	$I P/\gamma\beta$
Transverse resistive wall instability growth		1.6 μs	$I/\gamma\beta$
Control of spot size dilution due to kicker	√		none

From the table it is seen that the ETA-II experiments have lent considerable confidence to the DARHT 2 design. For example, the kicker operation

and control system performance have been demonstrated. There is reasonable confidence that the beam can be steered through the kicker and that the beam spot size can be adequately controlled as the beam traverses the downstream magnets. The amount of gas desorption from the septum is thought to be reliably extrapolated from the ETA experiments as well. However, the issues of background gas focusing as well as the suppression of the various instabilities will require future experiments on the 26 cell scaled DARHT accelerator with its 1.6 μ s pulse as well as, of course, on the complete DARHT facility.

6.8 Conclusions on Downstream Transport

Among the issues examined in this section, beam induced steering in the kicker, the amount of beam defocus caused by background gas as well as gas desorbed from the septum as the beam is kicked, the possibility of ion hose instability that results in the downstream region, the existence of transverse resistive wall instability, and the quality of the spot size due to the interaction of the beam with the kicker, only one seems a possible problem which needs to be addressed, ions backstreaming from the dump. All other issues appear to have been attended to very well, and in some cases represent well-studied physics with careful application to the parameters of DARHT 2.

Because there are four pulses sliced out of a long electron beam (1.6 μ sec long), it may be that enough ions produced at the beam dump early in the kicker sequence may reach the main beam axis to spatially broaden the last part of the long (1.6-2 μ sec) beam pulse and interfere with the quality of the later pulses sent to the target. In scaled experiments on DARHT this issue will be addressed, and we recommend that this also be studied carefully in simulations of the kicker-beam dump action in separating the long beam segment into four useful pulses for imaging the hydrodynamics.

7 TARGET ISSUES

The target remains one of the major technical challenges in the project. We were presented with the results of tests with two pulses, and four pulses are planned during the Scaled Accelerator Test. The principal problems are a) the disruption of the electron beam by back streaming ions from the target (with the faster light ions being worse), b) beam focusing by the thermal plasma in front of the target, and c) degradation and ultimate destruction of the target during the planned sequence of four pulses over 1.6 microsecond. Design of a target capable of meeting the project goals is difficult because all these problems require mitigation techniques which may themselves adversely impact performance; it is unclear how much design space – if any – exists in the midst of several countervailing effects.

We presented with promising results of feasibility studies using this approach carried out with two pulses on ETA. Given the technical challenges of using four pulses, additional tests are needed under these conditions. In this respect, we recommend straightforward and workable strategies such as the baseline approach. Four-pulse experiments are planned during the Scaled Accelerator Test and these will be of great importance in the development a successful target.

Effect b), beam focusing by the thermal plasma of heavy ions, remains the least studied effect, because it requires full DARHT 2 conditions to test properly. Project attention has been devoted mainly to the front side plasma, but plasma elsewhere is also worrisome. Simulations seem to show that the effect is not large enough to be greatly harmful to x-ray dose for the baseline design, but this cannot be demonstrated prior to the Scaled Accelerator Test.

Any of these approaches to ion and plasma suppression reduce the ultimate x-ray dose somewhat due to increased scattering of beam electrons; 50% reduction was quoted as a possibility. Project personnel expect that the de-

sign dose in each of the four pulses (100/100/100/300 rad) is still achievable, but this remains to be demonstrated.

Again, two-pulse tests have been performed and performance modeled (e.g., with LASNEX). This concept has not been proven; four-pulse tests need to be carried out to optimize geometries and materials to insure that the x-ray generation process in the initial pulse or two does not degrade the target during later pulses. Possible problems include plasma generation causing beam disruption, and shot-to-shot variation in the timing.

Though LASNEX is a code having a successful history and includes many physical effects, target simulation lies in a most challenging regime where plasma effects, electromagnetic effects, phase transitions, and strength of materials all play important roles, along with beam transport and hydrodynamics. For this reason, code results can only be used as a guide, and experiments with different target configurations will be essential to develop and validate a workable target.

The ETA test program has been useful and effective, within its restricted capabilities. Results of this program seem to show that there is high confidence in a two-pulse solution for the DARHT target. However the full physics of the four-pulse environment has not been addressed at ETA, so current confidence in a four-pulse solution is substantially lower; it will be essential to study it experimentally, which will be done in the Scaled Accelerator Test.

We conclude that the current baseline approach to target design has high confidence for delivery of two x-ray pulses, but only lower confidence for delivery of all four x-ray pulses meeting requirements. Promising approaches exist for a more capable target design, but will require further experimentation and development. The Scaled Accelerator Test is of key importance. Experiments therein must demonstrate mitigation of back streaming ions, control over the plasma cloud, and adequate target performance over four pulses.

8 USER PROGRAM

DARHT, already a key component of the U.S. hydrodynamic testing capability, will no doubt play an even more central role in the National Hydrotest Program over the coming years. DARHT 1 has been operational for several years, and DARHT 2 is scheduled to be operational in 2008. It is imperative that detailed plans be developed for its optimal use. We heard about initial planning for a user program, which is being developed despite the necessary focus on successfully commissioning DARHT 2. We did not hear of any details, however, either because they are not yet available or because our briefings were so focused on refurbishment of the machine. Still, recognizing that planning for the use of DARHT 2 may be further along than was reflected by the briefings, we offer some guidelines for developing a user program based on our experience with other major facilities.

The current schedule calls for an aggressive experimental program in FY 2006-2008 ramping up to begin use of DARHT 2 in FY 2009. In looking at limitations of the accelerator complex, we see nothing that would prevent a program with as many as one shot per week. Any limitations on test frequency are much more likely to come from infrastructure and support limitations for the experiments themselves.

These considerations imply that a coherent experimental plan should be in place for the full facility around the end of FY 2007, and a user program should be well underway by the end of FY 2008. In both cases, the timeline points to a start on developing both an experimental plan and a user program by the end of FY 2006. This not only allows appropriate preparation of budgets but also engages the current and future user community (DARHT's "customers") in the planning stages. This last point is important because inevitable tradeoffs will force decisions that need to be made wisely, and that also need to be absorbed into the culture of the interested technical

community. It is essential for the experimental community to work with weapon designers in establishing a plan of future experiments that will make best use of the facility. We have seen a general plan of experiments through FY 2010, based on the current understanding of programmatic needs for life extension programs and possible development of the RRW, though this plan will inevitably be adjusted as funding and other priorities are clarified.

We recommend developing an experimental plan based on technical considerations. The DARHT 2 performance parameters define a range of capabilities, including spatial and temporal resolution of images, reliability of 2- and 3-dimensional image reconstructions for various thicknesses of systems, and the like. These capabilities should be matched against the technical information that is needed with highest priority by the weapons designers, whether as part of surveillance, as needed for refurbishment or for other developments (e.g., RRW). It should be possible to express the designers' priorities in terms of QMU (Quantification of Margins and Uncertainties) metrics: that is, as enhancing the ratio of margins to their uncertainties as much as possible. In order to accomplish this, it is necessary to apply (and therefore develop, as needed) quantitative estimates based on the most advanced ASC simulations of how changes in specific radiographic observables translate into changes in yield or other measures of performance margins.

It is also important for the designers to establish a hypothesis-testing approach, such that experiments can support or refute quantitative expectations based on the current (evolving) state of understanding. Hypothesis testing can be prioritized in terms of how effectively an experiment will validate model simulations (or not), and in terms of the implications of the results for assuring the reliability, safety and performance of specific weapons. Both factors need to be considered, with sufficient agility to respond to unanticipated needs (e.g., from surveillance).

With this background, an overarching technically-based prioritization is then possible, whereby one convolves the prioritized needs of the designers with the quantitative capabilities of the facility in order to identify the set of experiments that can reveal the most important information most quickly. We have not seen such a plan, and have the impression that the weapon designers needs are not yet being effectively factored into the future scheduling of DARHT 2 experiments. While advocating that such technically-based planning begin over the coming months, we recognize that many other factors will also contribute to determining the ultimate schedule of experiments (e.g., LEP schedules set by external needs). Nevertheless, a technical analysis as we advocate here – determining a priority list of experiments based on matching technical needs and capabilities – will lead to optimal use of the facility when all considerations are taken into account.

Current practitioners of hydrotest experiments have considerable experience, in some cases including underground nuclear testing. As a user facility, however, DARHT cannot afford to focus only on such expert users, but should include supporting the next generation of experimentalists. That is, the users should be assumed to be naïve (albeit intelligent) in the specifics of the facility and in hydrotesting more generally. With this approach, DARHT can ensure most effective utilization of its facility by new as well as seasoned users. Moreover, DARHT would then also provide an important means of maintaining nuclear-weapons-related expertise.

In order to accomplish this goal, appropriate training and support infrastructure should be built into the user program right from the start. For example, training in safety and security measures, in target preparation and alignment, in carrying out shots (check lists, countdowns, etc.), and in data collection, archiving and analysis are among the pre-requisites of such a program. It is crucial that users understand not only what needs to be done, but also why – in general terms for all experimental activities, and in detail for those actions the person is responsible for carrying out.

Given that users have to be assumed to be away from their home base, it is important that adequate support facilities be provided: office space with access to e-mail and sufficient computational capability; support staff for promptly and clearly answering questions, or for making repairs and otherwise helping with experiments; and reasonable housing. The experimental laboratory should be flexible, so as to allow a wide variety of experiments and be able to respond to unexpected developments that are all too common with demanding experiments.

References

- [1] Briefing by Carl Ekdahl (LANL): “DARHT-II Long-Pulse Beam Dynamics”, 20 June 2006.
- [2] Y. Y. Lau, Phys. Rev. Letters **63**, 1141 (1989).
- [3] T. C. Genoni and T. P. Hughes, Phys. Rev. ST-AB **6**, 030401 (2003).
- [4] G. A. Travish, Transverse Beam Break-up in Linear Electron Accelerators, LBNL Report, January, 1990
- [5] Yu-Jiauan Chen, et al., Downstream Transport System for the Second Axis of the Dual-Axis Radiographic Hydrodynamic Test Facility, 14th International Conference on High-Power Particle Beams, AIP, 2002
- [6] M. J. Burns, et al., Status of the Dual Axis Radiographic Hydrodynamics Test (DARHT) Facility, 14th International Conference on High-Power Particle Beams, AIP, 2002
- [7] Briefing to JASON by G. J. Caporaso (LLNL) and Y. J. Chen (LLNL), “DARHT 2nd Axis Downstream Transport Design, Validation and Testing”, June 20, 2006.
- [8] J. F. McCarrick, A Study of the Ion Hose Instability in the DAHRT-II Downstream Transport Region, UCRL-TR-208591, December 15, 2004.
- [9] G. J. Caparaso and J. F. McCarrick, “Ion Hose Instability in a Long Pulse Induction Accelerator,” Proc. XX Int. Linac Conf., Monterey, CA, Aug 21-25, 2000, p.500
- [10] Prelas, M. A., Popovici, G. & Bigelow, L. K. Handbook of Industrial Diamonds and Diamond Films (Marcel Dekker, New York, 1998).

A APPENDIX: NNSA's Charge to JASON

The Conference Report for the Energy and Water Development Appropriations Act for FY 2006 (Public Law No: 109-103) states:

The conferees direct the JASONS to undertake a study of the Dual Axis Radiographic Hydro Test Facility (DARHT) to evaluate the DARHT 2nd axis refurbishment plan and to validate the current schedule and cost baseline. The conferees expect the JASONS to consider whether or not the NNSA has taken the appropriate steps to resolve the technical difficulties associated with the induction linac technology and whether or not the second axis is expected to return to service as currently planned in 2008 in order to meet the National Hydrotest Plan requirements.

While it is recognized that JASON has considerable technical expertise with which to review technical approaches, JASON has neither the time nor resources to do an in depth review of the accuracy of the cost accounting for the project, which has been reviewed in depth by an External Independent Review conducted by the DOE Office of Engineering and Construction Management. Recognizing this, the NNSA requests that JASON address the following issues over the course of the 2006 summer study:

1. Is there a sound technical basis for confidence in the refurbishment plans for the induction cells?
2. Is the approach to understanding beam stability issues and commissioning the accelerator technically sound?
3. Are there unaddressed technical risks for the LINAC or ancillary and support equipment to meet design performance requirements for the LINAC?

4. Is the technical approach to commissioning the downstream transport system sound?
5. What level of confidence exists that the 2nd axis will provide a useful multipulse capability? What risks remain in achieving the full 4-pulse capability at usable radiographic doses?
6. Does the project execution plan follow a clear logic that addresses the activities needed to complete and commission the 2nd axis?
7. In developing the final cost and schedule baseline project are there any significant shortfalls or gaps in the proposed technical scope or significant misestimates of resource requirements?
8. Is there adequate planning to use the full capabilities of the two-axis multipulse radiographic system when the facility becomes available for experimental use?

Because of Congressional interest in this subject JASON will provide to the NNSA a summary letter report by 1 August 2006 indicating significant findings and recommendations. A full report will be published subsequently.

B APPENDIX: Briefers

AGENDA

DARHT JASON REVIEW June 19 – 21, 2006

June 19, Monday

1:00 1:15	Welcome and Introduction	Charles McMillan
1:15 2:15	DARHT Project Overview	Ray Scarpetti
2:15 2:30	Break	
2:30 4:00	Requirements for Multi-pulse Radiology (U)	Maurice Sheppard

June 20, Tuesday

10:00 10:45	Cell Design, Testing and Refurbishment	Kurt Nielsen
10:45 11:05	Cell Refurbishment Process	Juan Barraza
11:05 12:20	Long-pulse Beam Dynamics	Carl Ekdahl
12:20 1:15	Lunch	
1:15 2:30	Downstream Transport Design, Validation and Testing	George Caporaso Yu-Jiuan Chen
2:30 2:45	Break	
2:45 4:15	Target Physics, Validation and Testing	Gary Guethlein

June 21, Wednesday

10:00 11:00	Injector Performance	Ben Prichard
11:00 11:30	Planning, Project Cost, Schedule, and Controls	Dan Jones
11:30 12:00	Summary and Conclusions	Ray Scarpetti
12:00 1:00	Lunch	
1:00 2:00	From Project Completion to a Dual Axis Radiographic Hydro Test facility	Rollin Whitman

C APPENDIX: Compensating for a lower DARHT 2 Current

The specifications for DARHT 2 do not include x-ray dose requirements. However, since producing x-ray dose is the purpose of the machine and sets the current requirements for a given pulse length, dose goals have been set. These are for the four temporally-separated pulses 100, 100, 100, and 300 Rads each, measured at 1 m from the x-ray conversion target. According to the baseline operational plan, the current required to achieve these dose levels is 2 kA, which is one of the specifications of the DARHT 2 project. At present, problems in the DARHT 2 injector have limited the current delivered to about 1 kA. The project team has confidence that the 2 kA current will be reached through improvements in the dispenser cathode that they plan to demonstrate within the next few months. However, at this point, the solution to the current problem remains a project uncertainty, raising the question of how serious a current limited to 1 kA would be, and what measures, if any, are available to compensate for the radiographic effect of operating at a reduced current.

First, it should be made clear that the expectation of improving cathode performance is reasonable based on past experience with dispenser cathodes. However, in answer to the worst-case question, there are two conceptual approaches to maintaining the radiographic capability at a current as low as 1 kA. The first is to improve the quantum efficiency of the detector, which would directly compensate for a lower dose. The second is to increase the temporal pulse width of each of the four pulses, since dose is also directly proportional to pulse width.

The first approach is really not feasible, as will be explained. The second, however, could readily be done with little impact on the project.

C.1 The Detector

When the DARHT project started, radiographic images were recorded on film, which, with enhancing metal screens, had a quantum efficiency of about one percent, meaning that 99% of the x-rays that penetrated the object, which were produced at high machine cost, did not contribute to the image. The efficiency was increased to a few percent by using multiple layers of film, but resolution degradation limited the number of layers that could be used. In addition, the requirement of DARHT 2 for recording four images in rapid succession precluded the use of film, requiring the development of an active detector. Detector requirements were:

- High quantum efficiency, which translated to
 - High Z for a large absorption coefficient
 - High density, to minimize the thickness requirement of the detection material and hence, the resolution degrading lateral scattering effects
- Efficient conversion of absorbed energy to optical photons to preserve quantum efficiency (Although different conversion mechanisms could, in principal, be chosen, in practice optical conversion was found to be the most promising.)
- Optical transparency
- Short time response ($< \sim 100$ ns) to prevent the overlap of images
- Segmentable material (as the large thickness requirements for high quantum efficiency would otherwise have unacceptable effects on image resolution), and for optimal results, segments that are in a conical pattern with the focus of the cone at the x-ray target.

The detector produced in the DARHT 2 project is very close to optimal, to the point that seeking further improvements to compensate for lower dose is impractical. The detector material is Lutetium oxyorthosilicate ($\text{Lu}_2\text{SiO}_5:\text{Cs}$). The characteristic of the material/detector are as follows:

- Z number (of Lu) = 71
- Density = 7.4 g/cm^3
- Thickness (length of segments) = 4 cm
- Optical conversion efficiency = 30,000 photons/MeV (i.e., 1 photon/33 eV)
- Quantum efficiency with DARHT 2 x-ray spectrum = 40%
- Optical decay time constant = 40 ns
- Fabricated into 0.9 mm segments, a size chosen so that the resolution contribution of the detector with the magnification of the experiment (M=4) would be less than the resolution effect of the radiographic spot size

These specifications are very good, allowing efficient optical coupling to the solid-state multi-image camera, which was also specially fabricated under the project to meet DARHT 2 requirements. It is very unlikely that the 40% quantum efficiency can be significantly improved on, given that the x-rays being detected are very penetrating, as they must be to image the thick implosions systems that are the purpose of DARHT 1 and DARHT 2.

C.2 Pulse Width of the Four DARHT 2 Pulses

The pulse widths that correspond to the dose goals for the four DARHT 2 pulses are 26, 26, 44, 100 ns. If the machine current was lowered from the projected 2 kA to 1 kA, the dose could be preserved by changing the pulse width format to 52, 52, 88, 200 ns, which is readily accomplished by simply adjusting the kicker power supply. The width of pulses is of importance in that the radiography must stop action of very fast moving phenomena. Typically explosively-driven hydrodynamic velocities are in the range of 1 μ s, which translates for a 200 ns interval to a motion of 0.2 mm, comparable to the resolution of the DARHT 2 radiographic system. However, speeds can be significantly amplified by convergence (i.e., shape charge jets, for which speeds can be up to 10 mm/ μ s), and DARHT 2 was designed such that hydrodynamic motion for any experiment of interest would not significantly increase blurring of the image. In the past, radiographic machines used for thick-object radiography have used pulse widths of up to 200 ns for hydrotests (PHERMEX and LLNL RF Linacs). A pulse width of 200 ns could introduce some motion blurring, but for most experiments, it would not be a large effect. In addition, DARHT 1, with a pulse width of 60 ns, and a dose that exceeds that of DARHT 2, would still provide superior stop action capability. Hence, while increasing the fourth pulse width to as much as 200 ns would be undesirable, it would not have a serious effect.

D APPENDIX: Simplified Simulation of DARHT Edge Resolution

So that we could have a better understanding of DARHT requirements, we undertook a simplified simulation of a typical radiography problem – in particular, of an image such as that which might be obtained by DARHT operating at 18 MeV through a thick section of uranium, hence with the most penetrating portion of the spectrum from 4-5 MeV X-rays. We took as a base case a 2 x 2 mm electron-beam target at a distance L from the object to be radiographed and a total distance ML from the camera. The magnification of the object is thus M , taken as 4 in this specific example.

A circular "aperture" 10 mm diameter in the object plane is imaged on the camera, where it forms a circle 40 mm in diameter.

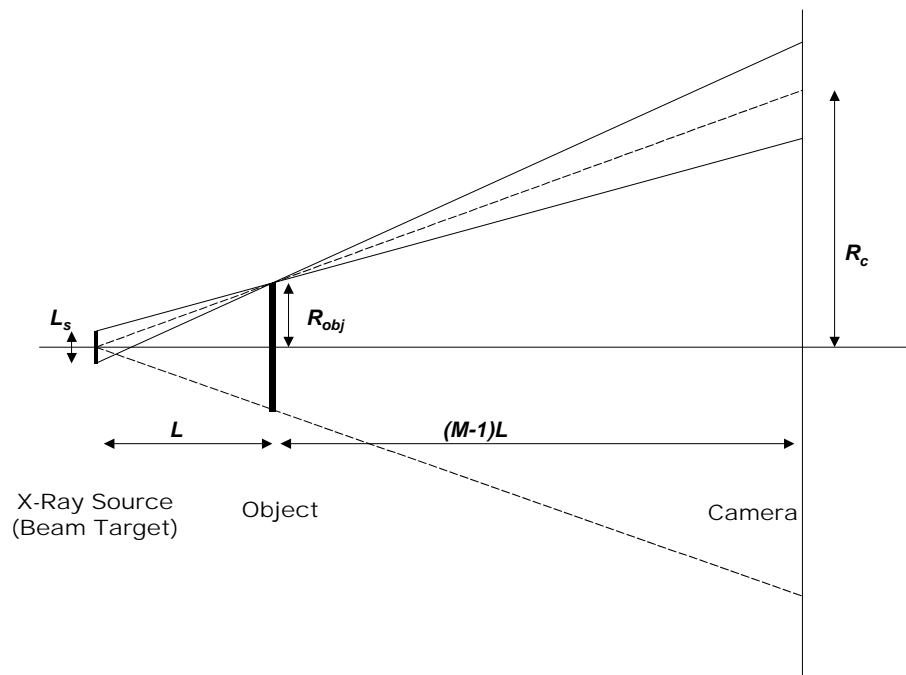


Figure D1. Transverse view of optical geometry that is simulated.

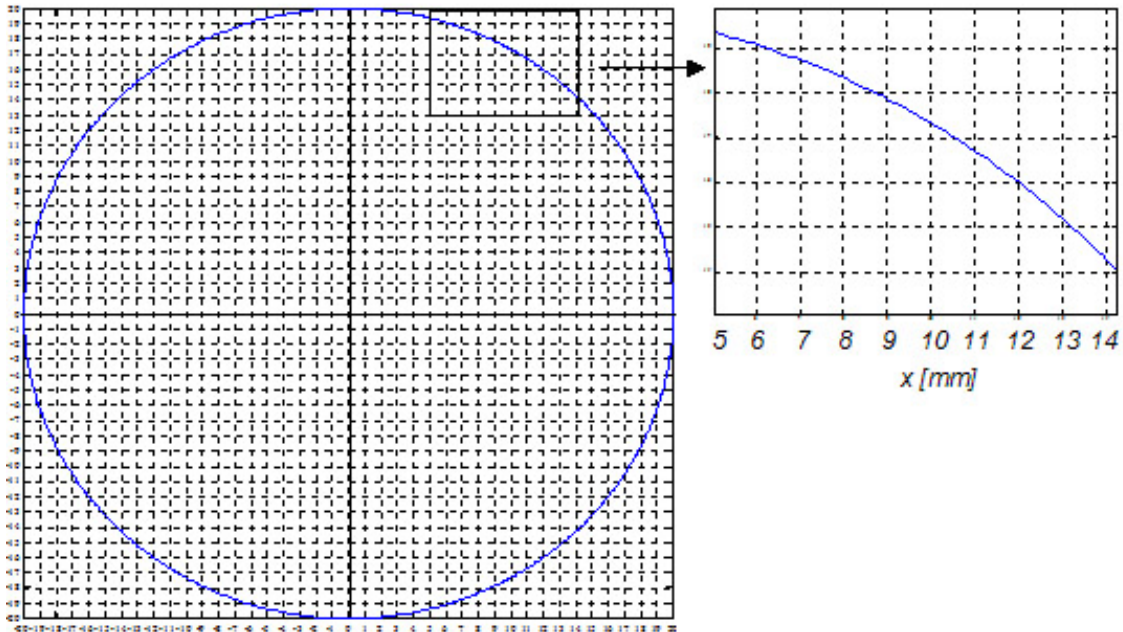


Figure D2. Projected circular image on a camera with 1mm x 1mm square pixels. Pixels within the analytically drawn curve are assigned a value of I_1 , and pixels outside are assigned a value of I_0 . Pixels that the curve intersects are assigned a value between I_1 and I_0 proportional to the fraction of the pixel that lies within the curve.

The image formed on the camera is rendered into 1mm x 1mm pixels by the simulation as described in figure D2. The result for a magnification of 4 and radius (R_c) of 20mm (on the camera) is shown in figure D3.

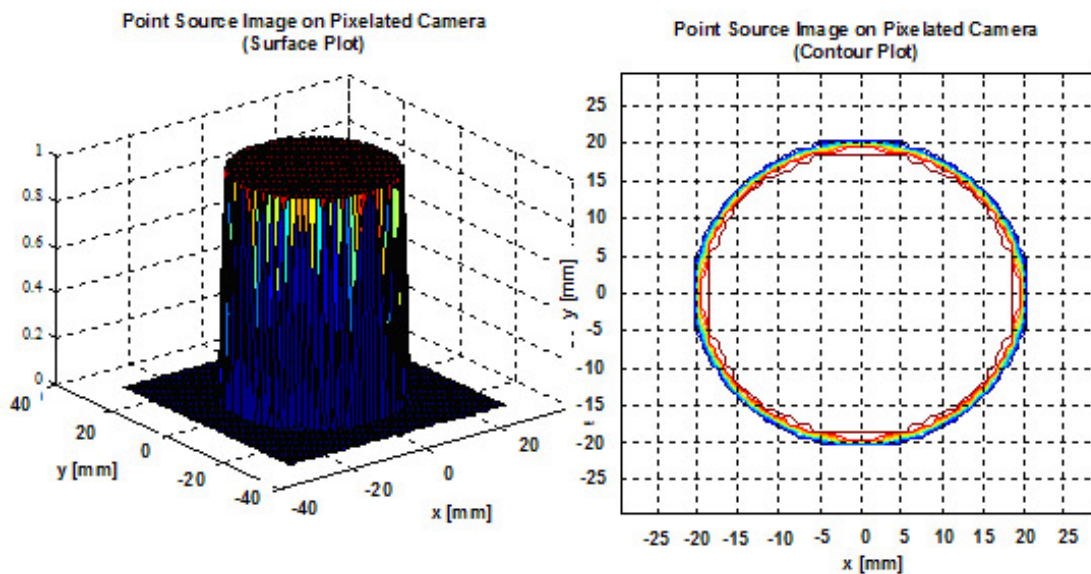


Figure. D3. Surface and contour plots of the image of circular object from point source of radiation on a camera of 1mm x 1mm pixels.

After accounting for pixelation of the point-source image we simulate the blurring effect of an extended radiation source by convolving the image of D3 with the projected image of the source on the camera. The result of convolution with a 6mm x 6mm image on the camera (corresponding to a 2mm x 2mm source) is given in figure D4.

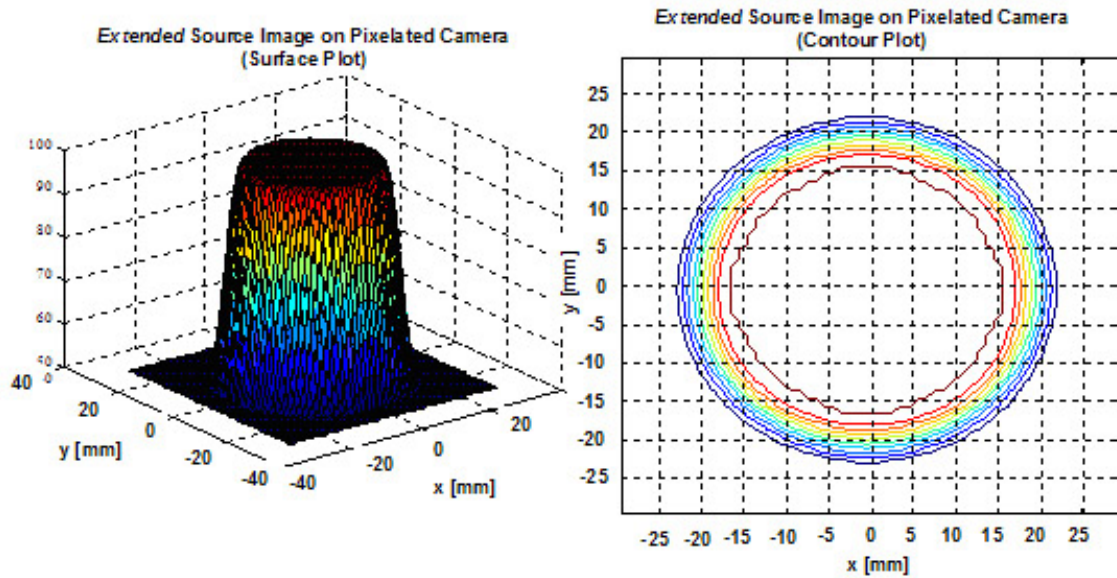


Figure D4. Image of circular object with blurring caused by extended source included, but no noise.

To model radiography through a thick layer of uranium, the image is simulated with 100 photons on each of the 1 x 1 mm detectors behind the aperture, and 50 photons detected per pixel behind the rest of the screen. Thus the image has a contrast ratio of 2, as would be caused by a cavity 5 mm deep in uranium of double normal density and a mass-absorption length of 22 g/sq cm.

One of the principal functions of radiography is to determine the precise location of interfaces in the object being radiographed. This could, for instance, be a spherical cavity, which would to some extent simulate the circular aperture. In fact, in this case we are simulating a cylindrical pillbox and a depth about 5 mm corresponding to 20 g/sq cm in uranium of density 40 g/cc.

Figure D5 shows the simulation of the image with shot noise added. To simulate shot noise, each pixel that has N photons has added to it a random number from a Gaussian distribution with a root-mean-square variation of $N^{1/2}$.

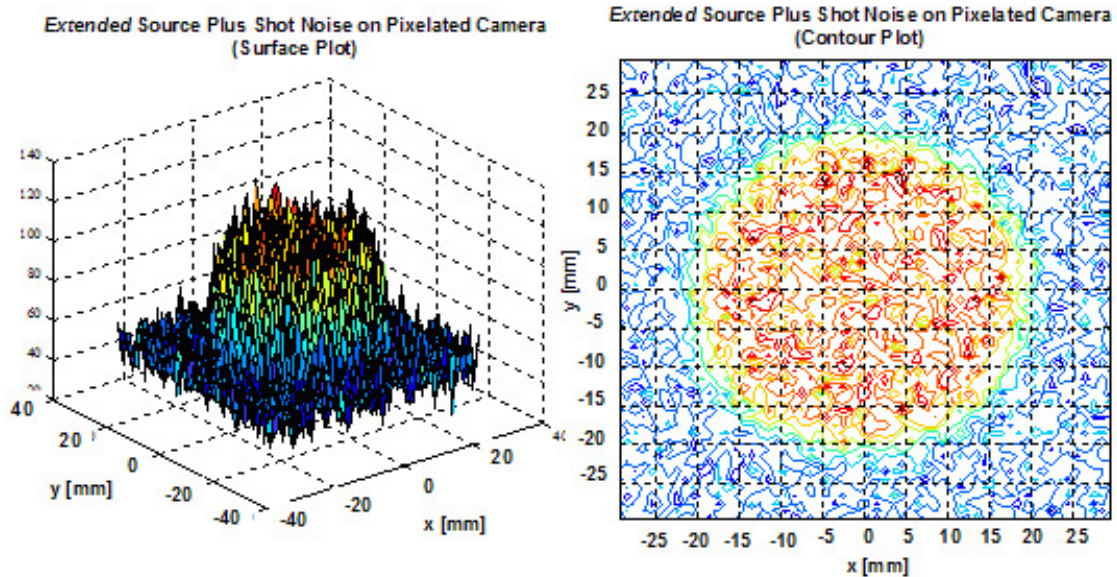


Figure D5. Surface and contour plots of the image of a circular object with both simulated shot noise and blurring caused by the extended source.

The eye normally fits the best smooth curve to the interface, which in this case approximates a circle. The derived radius of the circle in this way (for best fit) is far more accurate than is a single "line-out" plot of intensity as a function of distance, pixel by pixel along a radial line.

The simulation mimics the "fitting" of the eye by comparing the noisy image data against a candidate image that is generated by convolving the same "blurring matrix" with the point-source image of a sharp-edged aperture. The dimension(s) of the projected image of the aperture are varied (but holding the dimensions of the blurring matrix constant) until the best fit between the test image and the noisy data image is obtained. Two different kinds of candidate images were used for fitting. The first was a circle whose only changeable parameter was its radius, R_c . The second was an ellipse of fixed orientation, which had two changeable parameters, the semimajor and semiminor axes, a and b , respectively.

By simulating many (100) noisy circular images, each with a different noise field taken from the same distribution, a set of best-fit radii are obtained by fitting a given

circular candidate image to each simulated image. From these 100 fits the standard deviation best-fit radii can be observed. Fitting an *elliptical* candidate image to the same set of simulated data images a set of best-fit semimajor and semiminor axes lengths are obtained as well, from which standard deviations were calculated. These data are presented in Table **D1** as the standard deviation of the fit of a candidate image to the simulated, noisy image.

Table D1. Standard deviation of fit parameters obtained by fitting noise-free circular and elliptical candidate images to simulated data (with noise field) for four different types of extended sources (100 photons / pixel = "100% flux" here). Standard Deviation values were calculated over 100 runs. The precision obtained by these two-dimensional fits is significantly better than that obtained by the simple "line-out" approach.

	column 1	column 2	column 3	column 4
Source:	2x2mm (100% flux) σ [um]	1x1mm (100% flux) σ [um]	1x1mm (25% flux) σ [um]	1x4mm (100% flux) σ [um]
Rc	46	36	64	54
a	78	66	110	105
b	80	58	111	78

Column 1 in the table represents the standard deviation of the radius of the best-fit circle under the specified intensity conditions for the planned DARHT target 2mm x 2 mm, which produces at the camera a sloping edge of width $(M-1)T$, where T is the breadth of the target -- here 2 mm -- so that the projected image edge width is $(4-1)*2$ mm = 6 mm.

Simple analysis shows that if the target is uniformly illuminated and replaced by a 1mm x 1mm target that intercepts only 1/4 as much of the electron beam, the ramp will be half as wide, but the overall number of photons per detector element will be 1/4 as large (25 photons / pixel). According to the simple line-out model of resolution and for a camera of perfect resolution (zero pixel size), this should give a best-fit radius with a standard deviation just about what is available with the 2mm x 2mm target. Column 3 in the table provides the results for this simulation where we observe a slightly higher standard deviation of the fit values. This is in part a demonstration of the pixel pitch of the camera, but we have not fully explained these results.

DARHT does other things besides determining accurately the position of an interface. For instance, the depth of the cavity might be of interest, and that has very little to do with the resolution, but much more to do with the accuracy of determination of image intensity. We do not analyze that here, but realize that it should be the same with a 4mm x 1mm target as with the 2 x 2 mm target, assuming that the DARHT e-beam

diameter is sufficiently large to illuminate the 4-mm dimension. If it isn't, the beam can easily be distorted to do this.

Now the image of the circle will not be axisymmetric but will have an edge that is 3-mm wide along one axis and 12 wide along the perpendicular axis as seen in figure D6. The simulation models this, and the best-fit radius of the object circle (or ellipse) is determined in the same way as for the symmetric extended sources.

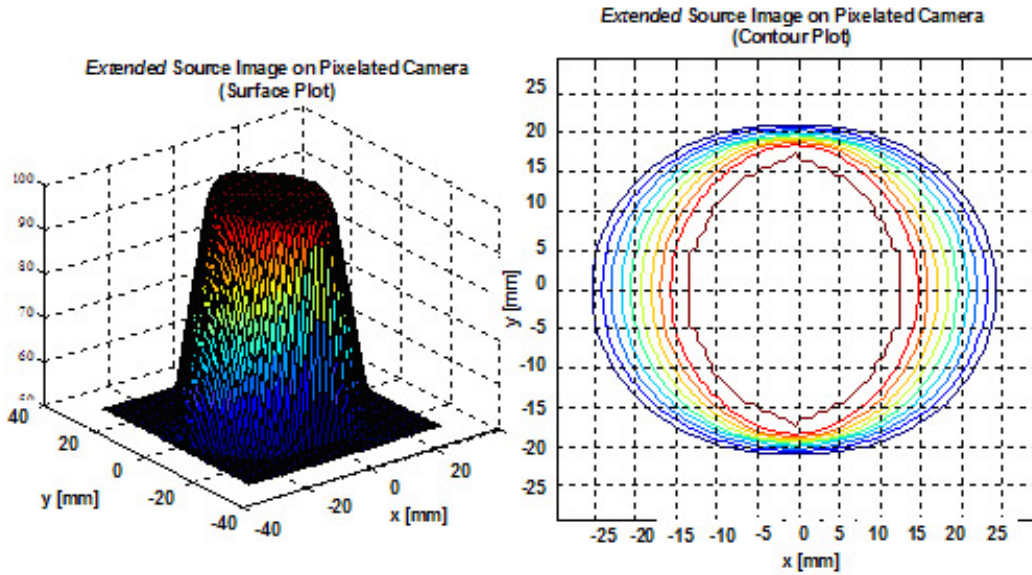


Figure D6. Image blurred by asymmetric extended source (4mm x 1mm). No noise field was included in this simulated image.

These multiple runs were then redone at a beam intensity five times smaller (20 photons / pixel), which should result in relative noise levels 2.2 times larger ($5^{1/2}$) and correspondingly larger fitting errors.

Table D2. Standard deviation of fit parameters obtained by fitting circular and elliptical test images to simulated data for four different types of extended sources with beam flux at 1/5 of previous results (20 photons / pixel = "100% flux" here). Standard deviation values were calculated over 100 runs.

	column 1	column 2	column 3	column 4
Source:	2x2mm (100% flux)	1x1mm (100% flux)	1x1mm (25% flux)	1x4mm (100% flux)
	σ [um]	σ [um]	σ [um]	σ [um]
Rc	107	74	137	122
a	186	140	259	273
b	192	125	240	181

Finally, one must make a connection between the 100 photons per detector assumed in these simulations and the 100 rad that is standard for one of the pulses of DARHT-2 incident on the object. One rad is defined as that radiation field that deposits 100 erg/g in water. Thus 100 rad deposits 10^4 erg/g of water, and the attenuation length for 5-MeV photons is 60 g/sq cm. The incident energy must then be 60×10^4 erg/g or 6×10^5 erg/sq cm. A 5-MeV photon that has maximum penetrating power in uranium has energy 8×10^{-6} erg, so there are $(6 \times 10^5)/(8 \times 10^{-6}) = 0.75 \times 10^{11}$ photon/sq cm or 0.75×10^9 photon/sq mm incident on the object.

The photon intensity at the object will be reduced by absorption/scattering attenuation and by geometry before reaching the camera. To determine geometrical decrease in photon intensity incident on the camera per unit area, we divide the photon intensity at the object by the square of the magnification, so $0.75 \times 10^9 / 16 = 4.68 \times 10^7$ photon/sq mm would be incident on the camera if no attenuation were present. Since our simulation assumes that the camera detects 100 photons per square millimeter within the "aperture," and since the detector's quantum efficiency is 0.4, the photon intensity (after attenuation) on the camera must be 250 photons per square millimeter to match the simulation. Thus the assumed attenuation before the object plane is $4.68 \times 10^7 / 250$ or 1.88×10^5 .

Since the absorption length in uranium is about 22 g/sq cm at 5 MeV, this factor 1.88×10^5 corresponds to just about $\ln(1.88 \times 10^5) = 12.14$ absorption lengths or about $22 \times 12.14 = 267$ g/sq cm.

If we relax the resolution requirements from the 46 μ m result of modeling with the 2x2mm source to 250 μ m (lowered by a factor of 5.43) then the fluence could be lower by a factor of 5.43^2 or 29.49. This increased tolerance would allow radiography through an additional $\ln(29.49) \times 22$ g/sq cm = 74.48 g/sq cm for a total of $267 + 74.5 = 341.5$ g/sq cm. This is indeed a very thick slab of uranium, but it does show the capability of a machine like DARHT.

The MATLAB code used in these simulations is available for the use of anyone who wants to verify it or to create his or her own simulation beginning with this approach.

DISTRIBUTION LIST

Director of Space and SDI Programs
SAF/AQSC
1060 Air Force Pentagon
Washington, DC 20330-1060

U S Army Space & Missile Defense Command
Attn: SMDC-ZD (Dr. Swinson)
PO Box 1500
Huntsville, AL 35807-3801

DARPA Library
3701 North Fairfax Drive
Arlington, VA 22203-1714

Department of Homeland Security
Attn: Dr. Maureen McCarthy
Science and Technology Directorate
Washington, DC 20528

Assistant Secretary of the Navy
(Research, Development & Acquisition)
1000 Navy Pentagon
Washington, DC 20350-1000

Principal Deputy for Military Application [5]
Defense Programs, DP-12
National Nuclear Security Administration
U.S. Department of Energy
1000 Independence Avenue, SW
Washington, DC 20585

Superintendent
Code 1424
Attn: Documents Librarian
Naval Postgraduate School
Monterey, CA 93943

Strategic Systems Program
Nebraska Avenue Complex
287 Somers Court
Suite 10041
Washington, DC 20393-5446

Headquarters Air Force XON
4A870 1480 Air Force Pentagon
Washington, DC 20330-1480

Defense Threat Reduction Agency [6]
Attn: Dr. Mark Byers
8725 John J. Kingman Rd
Mail Stop 6201
Fort Belvoir, VA 22060-6201

IC JASON Program [2]
Chief Technical Officer, IC/ITIC
2P0104 NHB
Central Intelligence Agency
Washington, DC 20505-0001

JASON Library [5]
The MITRE Corporation
3550 General Atomics Court
Building 29
San Diego, CA 92121-1122

U. S. Department of Energy
Chicago Operations Office Acquisition and
Assistance Group
9800 South Cass Avenue
Argonne, IL 60439

Dr. Jane Alexander
Homeland Security: Advanced Research
Projects Agency, Room 4318-23
7th & D Streets, SW
Washington, DC 20407

Dr. William O. Berry
ODUSD(ST/BR)
Acting Deputy Under Secretary of Defense for
Laboratories and Basic Sciences
875 N. Randolph Street
Arlington VA 22203

Dr. Albert Brandenstein
Chief Scientist
Office of Nat'l Drug Control Policy Executive
Office of the President
Washington, DC 20500

Ambassador Linton F. Brooks
Under Secretary for Nuclear Security/
Administrator for Nuclear Security
1000 Independence Avenue, SW
NA-1, Room 7A-049
Washington, DC 20585

Dr. James F. Decker
Principal Deputy Director
Office of Science
SC-2/Forrestal Building
U.S. Department of Energy
1000 Independence Avenue, SW
Washington, DC 20585

Ms. Shirley A. Derflinger
Management Analysis
Office of Biological & Environmental Research
Office of Science
SC-23/Germantown Building
U.S. Department of Energy
1000 Independence Ave., SW
Washington, D.C. 20585-1290

Dr. Martin C. Faga
President and Chief Exec Officer
The MITRE Corporation
Mail Stop N640
7515 Colshire Drive
McLean, VA 22102-7508

Mr. Dan Flynn [5]
Program Manager
DI/OTI/SAG
5S49 OHB
Washington, DC 20505

Dr. Paris Genalis
Deputy Director
OUSD(A&T)/S&TS/NW
The Pentagon, Room 3D1048
Washington, DC 20301

Mr. Bradley E. Gernand
Institute for Defense Analyses
Technical Information Services, Room 8701
4850 Mark Center Drive
Alexandria, VA 22311-1882

Dr. Lawrence K. Gershwin
NIC/NIO/S&T
2E42, OHB
Washington, DC 20505

U.S. Dept of Energy
National Nuclear Security Administration
1000 Independence Avenue, SW
NA-10 FORS Bldg
Washington, DC 20585

Mr. Hal Hagemer
Operations Manager
National Security Space Office (NSSO)
PO Box 222310
Chantilly, VA 20153-2310

Dr. Robert G. Henderson
Staff Director
The MITRE Corporation
Mailstop MDA/ Rm 5H305
7515 Colshire Drive
McLean, VA 22102-7508

Deputy Under Secretary
of Defense Science & Technology
3040 Defense Pentagon
Washington, DC 20301-3040

Dr. Bobby R. Junker
Office of Naval Research
Code 31
800 North Quincy Street
Arlington, VA 22217-5660

Dr. Andrew F. Kirby
DO/IOC/FO
6Q32 NHB
Central Intelligence Agency
Washington, DC 20505-0001

Dr. Anne Matsuura
Air Force Office of Scientific Research (AFOSR)
Program Manager, Atomic & Molecular Physics
875 N. Randall Street
Suite 235, Room 3112
Arlington, VA 22204

Dr. Daniel J. McMorro
Director, JASON Program Office
The MITRE Corporation
Mailstop T130
7515 Colshire Drive
McLean, VA 22102-7508

Dr. Julian C. Nall
Institute for Defense Analyses
4850 Mark Center Drive
Alexandria, VA 22311-1882

Mr. Thomas A. Pagan
Deputy Chief Scientist
U.S. Army Space & Missile Defense Command
PO Box 15280
Arlington, Virginia 22215-0280

Dr. John R. Phillips
Chief Scientist, DST/CS
2P0104 NHB
Central Intelligence Agency
Washington, DC 20505-0001

Records Resource
The MITRE Corporation
Mail Stop D460
202 Burlington Road, Rte 62
Bedford, MA 01730-1420

Dr. John Schuster
Submarine Warfare Division
Submarine, Security & Tech Head (N775)
2000 Navy Pentagon, Room 4D534
Washington, DC 20350-2000

Dr. Ronald M. Sega
Under Secretary of Air Force
SAF/US
1670 Air Force Pentagon
Room 4E886
Washington, DC 20330-1670

Dr. Alan R. Shaffer
Office of the Defense Research and Engineering
Director, Plans and Program
3040 Defense Pentagon, Room 3D108
Washington, DC 20301-3040

Dr. Frank Spagnolo
Advanced Systems & Technology
National Reconnaissance Office
14675 Lee Road
Chantilly, Virginia 20151

Mr. Anthony J. Tether
DIRO/DARPA
3701 N. Fairfax Drive
Arlington, VA 22203-1714

Dr. Jerry Elwood
Acting Associate Director of Science for
Biological and Environmental Research
Germantown Building / SC-23
U.S. Department of Energy
1000 Independence Avenue, S.W.
Washington, DC 20585-1290

Dr. Bruce J. West
FAPS - Senior Research Scientist
Army Research Office
P. O. Box 12211
Research Triangle Park, NC 27709-2211

Dr. Linda Zall
Central Intelligence Agency
DS&T/OTS
3Q14, NHB
Washington, DC 20505-00